JACS
JOURNAL OF THE AMERICAN CHEMICAL SOCIETY
Communication
pubs.acs.org/JACS

Lipoprotein Nanoplatelets: Brightly Fluorescent, Zwitterionic Probes with Rapid Cellular Entry

Sung Jun Lim,[†,‡] Daniel R. McDougle,[§,∥] Mohammad U. Zahid,[†,‡] Liang Ma,[‡,⊥] Aditi Das,[*,†,§,#,⊗] and Andrew M. Smith[*,†,‡,⊥]

[†]Department of Bioengineering, [‡]Micro and Nanotechnology Laboratory, [∥]College of Medicine, [⊥]Department of Materials Science and Engineering, [#]Department of Biochemistry, [⊗]Beckman Institute for Advanced Science and Technology, University of Illinois at Urbana−Champaign, Urbana, Illinois 61801, United States

[§]Department of Comparative Biosciences, University of Illinois at Urbana−Champaign, Urbana, Illinois 61802, United States

Supporting Information

ABSTRACT: Semiconductor nanoplatelets (NPLs) are planar nanocrystals that have recently attracted considerable attention due to their quantum-well-like physics, atomically precise thickness, and unique photophysical properties such as narrow-band fluorescence emission. These attributes are of potential interest for applications in biomolecular and cellular imaging, but it has been challenging to colloidally stabilize these nanocrystals in biological media due to their large dimensions and tendency to aggregate. Here we introduce a new colloidal material that is a hybrid between a NPL and an organic nanodisc composed of phospholipids and lipoproteins. The phospholipids adsorb to flat surfaces on the NPL, and lipoproteins bind to sharp edges to enable monodisperse NPL encapsulation with long-term stability in biological buffers and high-salt solutions. The lipoprotein NPLs (L-NPLs) are highly fluorescent, with brightness comparable to that of wavelength-matched quantum dots at both the ensemble and single-molecule levels. They also exhibit a unique feature of rapid internalization into living cells, after which they retain their fluorescence. These unique properties suggest that L-NPLs are particularly well suited for applications in live-cell single-molecule imaging and multiplexed cellular labeling.

Semiconductor nanocrystals are the subject of extensive multidisciplinary studies due to their unique physical, optical, and electronic properties.[1] Their primary emergent property is bright, stable fluorescence emission that is tunable across a broad range of wavelengths. This characteristic has enabled diverse applications as imaging agents and molecular probes in cells and tissues[1a] and as light-emitting components of diodes and display devices.[1b,c] These particles are especially useful in single-molecule imaging applications, where their unique combination of high photon emission rate and compact size has facilitated the discovery of a host of new biomolecular phenomena.[2]

Prototypical semiconductor nanocrystals are quasi-spherical quantum dots (QDs) and elongated nanorods (NRs).[3] Recently a new class of material has emerged, called nanoplatelets (NPLs), with a variety of unusual structural and optical properties.[3b,4] NPLs are thin crystalline sheets with atomically flat surfaces, tunable from 1.2 to 2.8 nm in thickness,[4a,5] and roughly 5−700 nm in lateral dimensions;[6] thus, they are colloidal analogues of quantum wells. Their fluorescence emission bandwidth is exceptionally narrow (8−20 nm full width at half-maximum, fwhm) compared to that of QDs (typically 25−35 nm fwhm) and organic fluorophores (typically 35−45 nm fwhm). Their light-collecting efficiency can be very large: a single CdSe NPL with 1.5 nm thickness and 30 nm lateral dimensions has a molar extinction coefficient near 5×10^7 M^{-1} cm^{-1}, roughly 1000× that of green fluorescent protein. In addition, unlike QDs, NPLs have high surface-area-to-volume ratios, which may facilitate efficient transfer of energy and charge and efficient modulation of their optical properties by changes in the local environment.[7] Together, these properties could allow multiplexed imaging with reduced spectral crosstalk as well as enhanced sensitivity for analyte detection. Recently, CdSe-based NPLs have been coated with CdS shells, resulting in greatly enhanced fluorescence quantum yield (QY),[8] a critical step forward in the production of bright NPLs suitable for imaging in oxidizing environments.

It is an outstanding current challenge to stabilize NPLs in aqueous solutions compatible with cells and tissues. Like QDs and NRs, these materials are synthesized in organic solvents and coated with aliphatic ligands (e.g., oleic acid) that render them insoluble in polar solvents. We found that conventional phase-transfer techniques used for core/shell CdSe/CdS QDs, such as ligand exchange with hydrophilic thiolates, can damage the NPL structure and/or quench fluorescence entirely (Figure S1).

Here we demonstrate the production of a new class of water-stable NPLs encapsulated in lipoproteins. These lipoprotein nanoplatelets (L-NPLs) derive from lipoprotein nanodiscs. Nanodiscs are nanoscale analogues of plasma membranes consisting of a phospholipid bilayer stabilized by helical, amphipathic membrane scaffold proteins (MSPs) that encircle the nanodisc like a belt.[9] Nanodiscs are used to solubilize integral and transmembrane proteins in aqueous solution and encapsulate hydrophobic drugs,[9c,10] suggesting that they may be able to encapsulate and stabilize NPLs in aqueous solution. Lipid-encapsulation is a versatile strategy to transform hydrophobic colloidal nanoparticles into biocompatible nanostructures,[11] but it is critical to geometrically match the nanoparticle morphology with the native self-assembled lipid structure to generate stable

Received: October 30, 2015
Published: December 19, 2015

DOI: 10.1021/jacs.5b11225
J. Am. Chem. Soc. 2016, 138, 64−67

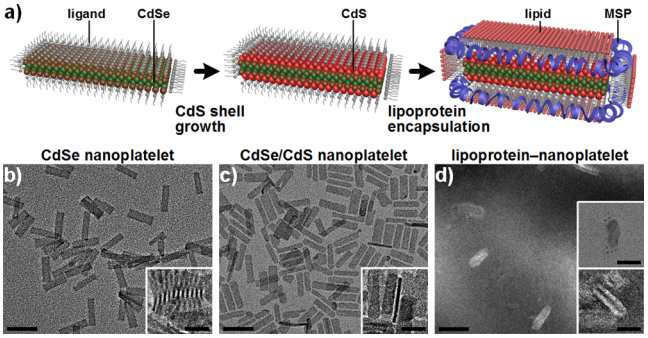

Figure 1. Synthesis and structure of lipoprotein nanoplatelets. (a) Schematic illustration of synthesis steps. TEM images depict (b) CdSe core NPLs (unstained), (c) CdSe/CdS core/shell NPLs (unstained), and (d) L-NPLs (counter-stained). Insets show side views of particles. Top inset in (d) shows L-NPLs after MSP conjugation to gold colloids. Scale bars = 50 nm in wide-field images and 20 nm in insets.

and individually coated nanoparticles. For example, spherical nanoparticles such as QDs and gold colloids are successfully encapsulated by amphiphilic polymers,[12] polyethylene glycol (PEG)-containing phospholipids,[11] and globular lipoproteins[13] that individually self-assemble into spherical colloids in water. This is due to a high volume ratio of the polar head domain to the nonpolar tail domain, or a large packing parameter, matching the high surface curvature of the encapsulated isotropic particles.[14] We found that PEG-phospholipids can encapsulate flat NPLs, but their fluorescence was entirely quenched, likely due to sparse lipid packing on the flat surfaces (Figure S1). Instead, lipids with small packing parameters are geometrically ideal for flat NPLs, but they have a tendency to form large liposomes entrapping multiple nanoparticles.[15] We hypothesized that nanodisc components, including phospholipids with packing parameters that yield flat structures and MSPs that stabilize truncated edges with high curvature, are ideal for NPL encapsulation.

L-NPLs were synthesized in a three-step process (Figure 1a) comprising colloidal synthesis of CdSe core NPLs, growth of a CdS shell, and encapsulation of CdSe/CdS core/shell NPLs in nanodisc components (Supporting Methods). CdSe was used for the core due to robust syntheses that allow independent tuning of lateral dimensions and thickness, as well as narrow-band fluorescence emission in the visible spectrum.[4a,5a] Figure 1b shows an example of uniform rectangular-shaped CdSe NPLs with 41×11 nm lateral dimensions and 1.8 nm thickness, measured by transmission electron microscopy (TEM; see statistics in Figure S2). These thin nanocrystals are flexible and form stacks of twisted NPLs (see inset). Layer-by-layer shell growth techniques were recently introduced for deposition of CdS, which has a wider bandgap (2.5 eV) than the core CdSe material (1.76 eV).[8] The shell boosts QY and allows better preservation of fluorescence in aqueous media (see below). Figure 1c shows that after 2 monolayers (ML) of growth, the lateral dimensions were similar (42×12 nm), but the thickness increased to 3.0 nm. Twisted and stacked NPLs were no longer observed (see inset) indicating that shell growth increased structural rigidity. Finally, these core/shell NPLs were encapsulated in lipoprotein nanodisc components through an evaporation−encapsulation process described below.[9b] Counter-stained TEM images (Figure 1d) show individual core/shell NPLs uniformly surrounded by a 3−4 nm organic coating (Figure S2), consistent with an inner layer of oleate ligands bound to the NPL surface and an outer layer of phospholipids and MSPs.

Efficient encapsulation of NPLs required three components: phospholipids, detergents, and MSPs (Figure S3). To generate L-NPLs, NPLs were dispersed in chloroform and self-assembled with excess phospholipids through slow solvent evaporation followed by dispersion in phosphate-buffered saline (PBS) containing a mixture of detergents (sodium cholate or *n*-decyl-*β*-maltoside) and amphipathic MSPs (e.g., MSP1E3D1). Zwitterionic phospholipids were used to optimize biocompatibility and dispersion stability, and were chosen to have a packing parameter near 1 for dense assembly on the flat NPL surfaces; we used 1,2-dimyristoyl-*sn*-glycero-3-phosphocholine (DMPC) or 1-palmitoyl-2-oleoyl-*sn*-glycero-3-phosphocholine (POPC). Eliminating any one of the three components significantly reduced the phase-transfer efficiency and stability of NPLs in aqueous solution. Phospholipids alone natively self-assemble into larger liposomal structures,[16] yielding a low percentage of NPLs transferred into aqueous buffer (most products were insoluble aggregates). Detergents dissociate liposomal structures into smaller metastable micelles;[16a] this increased the phase-transfer efficiency of NPLs, but aggregation was still substantial. Adding MSPs caused NPLs to readily disperse in water without substantial aggregates, yielding ≥33% of encapsulated NPLs that were stable for more >1 month after extensive dialysis and density gradient centrifugation in high salt (even >4 M NaCl) to remove empty nanodiscs and expel detergents (Figures S4 and S5). MSPs also eliminated fluorescence quenching from detergents that strip off oleate ligands from NPLs (Figure S6).

We characterized L-NPLs using multiple analytical methods and determined that the structure is consistent with Figure 1a, in which lipids cover flat NPL surfaces and MSP proteins adsorb to curved edges. For L-NPLs made from NPLs with average dimensions of 37×10×3 nm, it was determined that there was an average of 1193 DMPC lipids per NPL based on elemental analysis of cadmium (only in the CdSe/CdS NPL core) and phosphorus (only in the phospholipid). Assuming that DMPC adopts a similar area as in nanodiscs (0.69 nm^2 $DMPC^{-1}$),[9b] this quantity is consistent with a monolayer coating of the flat top and bottom of the NPL (740 nm^2 surface area, or 1070 lipids) and some of the sides (282 nm^2 surface area, or 409 lipids). The slight deficiency is likely covered by MSP proteins. We calculated an average of 7.7 MSPs per L-NPL by spectral analysis of L-NPLs prepared with dye-labeled MSP (Figure S7). MSPs likely localize to edges to interact with lipid tail sides where they reside analogously in nanodiscs. This is consistent geometrically, as MSP1E3D1 extends to a length of 38 nm in a nanodisc (circumference of a nanodisc with 13 nm diameter),[9b] so theoretically at least 5.0 MSPs are needed to cover both top and bottom edges of the NPL (total perimeter length of 188 nm), only slightly less than the measured value of 7.7. Deviations may arise from protein conformation differences on the circular nanodisc versus the rectangular NPL. This model was further justified by an imaging study to localize MSPs using TEM. We conjugated gold colloids activated with *N*-hydroxylsuccinimide (NHS) to L-NPLs. Because only the MSP protein contains primary amines with which NHS will conjugate, gold should only localize to the protein. TEM showed that NHS-gold was almost exclusively localized around the L-NPL perimeter, as opposed to the particle center (Figure 1d inset and Figure S8).

The optical properties of CdSe core and CdSe/CdS core/shell NPLs before and after coating with lipoprotein/MSP are shown in Figure 2. The crystalline CdS shell was necessary for maintaining fluorescence in water, as core-only NPLs completely quenched after lipoprotein/MSP encapsulation, despite a QY of 2.3% in

DOI: 10.1021/jacs.5b11225
J. Am. Chem. Soc. 2016, 138, 64−67

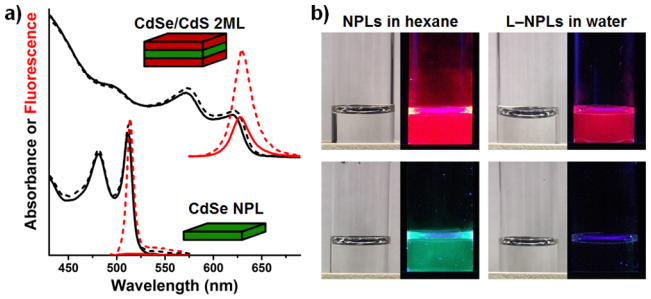

Figure 2. Optical properties of CdSe and CdSe/CdS L-NPLs. (a) Visible absorption (black) and fluorescence (red) spectra of CdSe core (bottom) and CdSe/CdS core/shell (top) NPLs in hexane (dotted lines) and corresponding L-NPL structures in PBS (solid lines). (b) Photographs of sample solutions under room light (left) or 366 nm lamp excitation (right).

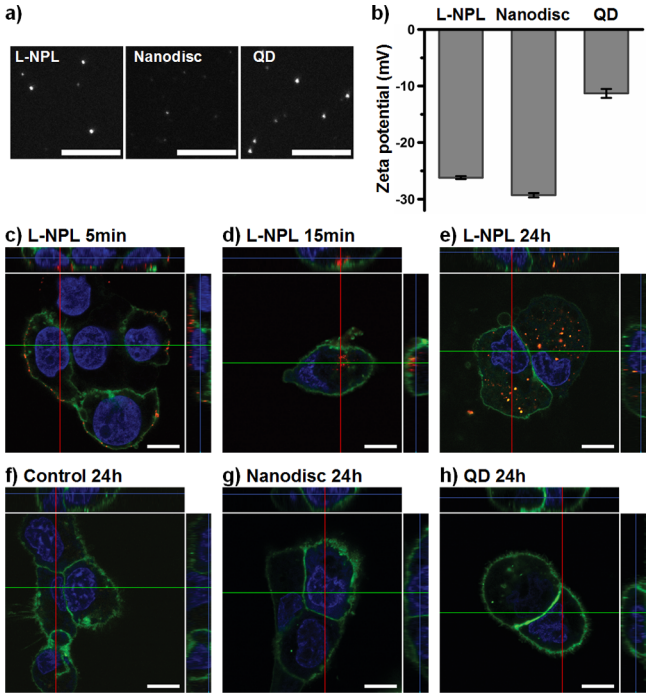

Figure 3. (a) Single-particle fluorescence images of L-NPLs, dye-labeled nanodiscs, and QDs, cast from aqueous solution. (b) Zeta potential measurements of the three samples. (c–h) Fluorescence confocal microscopy images of A431 cells as 3D z-stack projections of three color channels: blue = nuclear dye, green = membrane dye, and red = L-NPL, nanodisc, or QD. Duration of exposure to each nanoparticle is given for each image. Uptake was only significant for L-NPLs. All red channel images in panels c–h were acquired under identical imaging conditions. All scale bars = 10 μm.

organic solvents. With CdS shell growth, QY increased significantly in organic solvents, and could reach 80% with thick shells (7–8 ML).[8c] Unlike core-only NPLs, the fluorescence of core/shell NPLs was preserved after encapsulation, but the QY partially decreased in a manner dependent on the CdS shell thickness. For a 2-ML shell (the structure used in cells below) a 4.3% QY in hexane resulted in a 1.6% QY in water (Figure 2b, top). Thinner shells yielded more substantial QY loss while thicker shells provided greater QY retention. While a shell is necessary to maintain fluorescence, increasing thickness diminishes the unique optical attributes of NPLs as well as their potential for environmental sensitivity and flexibility. For example, CdSe-only NPLs have exceptionally narrow emission bands (fwhm = 9 nm for λ_{em} = 515 nm), but they monotonically broaden with shell growth, likely due to increasing structural heterogeneity or/and increased electron–phonon coupling.[8c] We find that at intermediate shell thickness (2–3 ML), bands are still narrower (fwhm = 21 nm at λ_{em} = 626 nm) than those of spectrally matched QDs (fwhm = 25–35 nm at λ_{em} = 600–650 nm), so we focused on this structural set for further investigations.

To investigate the potential of L-NPLs as fluorescent imaging probes, we measured their optical and diffusive behavior at the single-particle level using fluorescence microscopy. L-NPLs and QDs with similar emission wavelengths were spin-coated from dilute aqueous solutions on a glass coverslip. Individual emitters were distinguished by fluorescence intermittency (blinking) and homogeneous intensity levels in the blinking "on" state. L-NPLs exhibited longer "off" times and shorter "on" times (Figure S9). The "on" time brightness values were measured for at least 250 single particles using Lagerholm's method (Supporting Methods).[17] Average relative single-particle brightness values were similar for L-NPLs ($B_{rel,sp}$ = 2.06±0.98) and QDs ($B_{rel,sp}$ = 1.94±0.90), with L-NPLs being slightly brighter (by 6%). At the ensemble level, absolute brightness values were calculated from the relation B_{rel} = QY × ε, where ε is the extinction coefficient calculated from the particle core volume from TEM and the $CdSe_xS_{1-x}$ concentration derived from elemental analysis.[18] Ensemble brightness values were similar for L-NPLs ($B_{rel,en}$ = 4.0×10^5 cm^{-1} M^{-1}) and QDs ($B_{rel,en}$ = 4.7×10^5 cm^{-1} M^{-1}), with L-NPLs being slightly dimmer (by 14%). The small mismatch between ensemble and single-particle brightness values may originate from errors in extinction coefficient calculations due to structural anisotropy, the possible presence of "dark" L-NPLs not counted in single-particle analyses, or preferential alignment on the substrate. These results confirmed that L-NPLs are bright single-molecule emitters, comparable to QDs, but with narrower bandwidths.

L-NPL diffusion was probed through single-particle fluorescence imaging in dilute solutions. By fitting mean squared displacements of 429 single-particle trajectories to a model of Brownian motion, the mean center-of-mass diffusion coefficient was calculated to be 1.55±0.71 μm^2 s^{-1} in 50% (w/w) glycerol–sodium borate buffer (Figure S9). By the Stokes–Einstein equation, the diameter of an equivalent sphere is 46.1 nm, close to many QDs in common use and thus appropriate for cellular and molecular imaging applications.[19]

Finally, we investigated the interactions of L-NPLs with live A431 human epidermoid carcinoma cells to evaluate their potential for use as single-molecule imaging probes and cellular labels (Figure 3). We compared L-NPLs directly with two chemically analogous nanoparticles: empty nanodiscs composed of the same lipid/lipoprotein components labeled with a fluorophore (Texas Red) and zwitterionic QDs. All three had similar red emission wavelengths and were readily visible at the single-particle level under identical imaging conditions (Figure 3a). Zeta potential measurements in phosphate-buffered solution indicated that all nanoparticles were anionic. The L-NPLs and nanodiscs were similar (−25 to −30 mV), but the zwitterionic QDs, having no protein component, had a lower charge (−11 mV) (Figure 3b). At equal particle concentrations (1 nM), cells exposed to L-NPLs showed a much higher level of intracellular red fluorescence (Figure 3c–e) compared to control cells and cells exposed to nanodiscs or QDs (Figure 3f–h). We tracked this via confocal microscopy and stained cells with a nuclear dye (blue)

DOI: 10.1021/jacs.5b11225
J. Am. Chem. Soc. 2016, 138, 64–67

and a plasma membrane dye (green). We observed that internalization is rapid, with L-NPLs colocalizing with the membrane within 5 min of exposure, and becoming internalized within 15 min (see trend in Figure S10). After 24 h, uptake was substantial, consisting of bright punctate cytosolic spots of L-NPLs likely in endosomal vesicles. It is surprising that among three chemically similar particles, only L-NPLs exhibited substantial uptake. Zwitterionic components were shared by all particles, so they likely did not contribute. MSP protein was also not likely the contributor, since MSP-containing nanodiscs did not exhibit substantial uptake. A protein conformation change is also not likely the source, as the result was similar when MSP was PEGylated to block protein-mediated cell association (Figure S11). The strong uptake likely arises from the high surface area and low curvature of L-NPLs, for which multiple weak adsorption events can become substantial in strength through multivalency. Overall these observations suggest that L-NPLs are a promising class of fluorophore for intracellular imaging and for efficient fluorescence tagging of cells.

In conclusion, we engineered a new composite nanocrystal comprising a quantum-well-like nanoplatelet encapsulated within phospholipid and lipoprotein components of a nanodisc, yielding colloidally stable fluorophores with bright emission at the ensemble and single-particle levels. Employing geometrically compatible materials is critical, and extensive studies in nanodisc engineering[9,10] set the stage for diverse chemistries and biological functionality of L-NPLs. The unique shapes and optical properties of these materials are intriguing in the context of single-molecule imaging, optical cellular tagging, and even drug delivery, as high-aspect-ratio particles have been observed to have enhanced permeation through crowded tissues and unique delivery capabilities in living animals.[20] In fact, we expect that this new material composite will help reveal, at the single-particle level, how two-dimensional materials interact with biological systems. To our knowledge, these studies are the first example of a colloidal fluorescent quantum well employed in biological systems. The unique finding of rapid cellular entry suggests that these materials may be immediately useful for cellular labeling applications to allow highly multiplexed spectral encoding of cellular identity. Further studies are needed to assess whether cytotoxic effects of NPLs are enhanced due to their large surface areas compared with QDs and whether blinking rate differences can be controlled.

■ ASSOCIATED CONTENT

Supporting Information

The Supporting Information is available free of charge on the ACS Publications website at DOI: 10.1021/jacs.5b11225.

Supporting Methods and Figures S1−S11 (PDF)

■ AUTHOR INFORMATION

Corresponding Authors

*aditidas@illinois.edu

*smi@illinois.edu

Notes

The authors declare no competing financial interest.

■ ACKNOWLEDGMENTS

The authors acknowledge support from the NIH (A.M.S., R00CA153914 and R21NS087413; L.M., T32ES007326), the UIUC College of Engineering Strategic Research Initiatives Program, and the American Heart Association (D.R.M., 14PRE20130015; A.D., 15SDG25760064). We thank Ms. Yelena Grinkova, Dr. Mark McLean, and the Sligar lab for discussions and assistance with MSP production, and Core Facilities at the Carl R. Woese Institute for Genomic Biology for microscopy assistance.

■ REFERENCES

(1) (a) Kairdolf, B. A.; Smith, A. M.; Stokes, T. H.; Wang, M. D.; Young, A. N.; Nie, S. *Annu. Rev. Anal. Chem.* **2013**, *6*, 143. (b) Talapin, D. V.; Lee, J. S.; Kovalenko, M. V.; Shevchenko, E. V. *Chem. Rev.* **2010**, *110*, 389. (c) Mashford, B. S.; et al. *Nat. Photonics* **2013**, *7*, 407.

(2) (a) Zahid, M. U.; Smith, A. M. Single-Molecule Imaging with Quantum Dots. In *Optical Nanoscopy and Novel Microscopy Techniques*; Xi, P., Ed.; CRC Press: Boca Raton, FL, 2014; pp 135−160. (b) Pinaud, F.; Clarke, S.; Sittner, A.; Dahan, M. *Nat. Methods* **2010**, *7*, 275.

(3) (a) Smith, A. M.; Nie, S. *Acc. Chem. Res.* **2010**, *43*, 190. (b) Lim, S. J.; Smith, A.; Nie, S. *Curr. Opin. Chem. Eng.* **2014**, *4*, 137. (c) Fu, A.; Gu, W. W.; Boussert, B.; Koski, K.; Gerion, D.; Manna, L.; Le Gros, M.; Larabell, C. A.; Alivisatos, A. P. *Nano Lett.* **2007**, *7*, 179. (d) Yong, K. T.; Qian, J.; Roy, I.; Lee, H. H.; Bergey, E. J.; Tramposch, K. M.; He, S. L.; Swi-hart, M. T.; Maitra, A.; Prasad, P. N. *Nano Lett.* **2007**, *7*, 761.

(4) (a) Ithurria, S.; Tessier, M. D.; Mahler, B.; Lobo, R.; Dubertret, B.; Efros, A. *Nat. Mater.* **2011**, *10*, 936. (b) Bouet, C.; Tessier, M. D.; Ithurria, S.; Mahler, B.; Nadal, B.; Dubertret, B. *Chem. Mater.* **2013**, *25*, 1262.

(5) (a) Ithurria, S.; Dubertret, B. *J. Am. Chem. Soc.* **2008**, *130*, 16504. (b) Son, J. S.; et al. *Angew. Chem., Int. Ed.* **2009**, *48*, 6861.

(6) Bouet, C.; Mahler, B.; Nadal, B.; Abecassis, B.; Tessier, M. D.; Ithurria, S.; Xu, X. Z.; Dubertret, B. *Chem. Mater.* **2013**, *25*, 639.

(7) Rowland, C. E.; Fedin, I.; Zhang, H.; Gray, S. K.; Govorov, A. O.; Talapin, D. V.; Schaller, R. D. *Nat. Mater.* **2015**, *14*, 484.

(8) (a) Ithurria, S.; Talapin, D. V. *J. Am. Chem. Soc.* **2012**, *134*, 18585. (b) Mahler, B.; Nadal, B.; Bouet, C.; Patriarche, G.; Dubertret, B. *J. Am. Chem. Soc.* **2012**, *134*, 18591. (c) Tessier, M. D.; Mahler, B.; Nadal, B.; Heuclin, H.; Pedetti, S.; Dubertret, B. *Nano Lett.* **2013**, *13*, 3321.

(9) (a) Bayburt, T. H.; Grinkova, Y. V.; Sligar, S. G. *Nano Lett.* **2002**, *2*, 853. (b) Denisov, I. G.; Grinkova, Y. V.; Lazarides, A. A.; Sligar, S. G. *J. Am. Chem. Soc.* **2004**, *126*, 3477. (c) McDougle, D. R.; Palaria, A.; Magnetta, E.; Meling, D. D.; Das, A. *Protein Sci.* **2013**, *22*, 964. (d) Roy, J.; Pondenis, H.; Fan, T. M.; Das, A. *Biochemistry* **2015**, *54*, 6299.

(10) (a) Bayburt, T. H.; Grinkova, Y. V.; Sligar, S. G. *Arch. Biochem. Biophys.* **2006**, *450*, 215. (b) Das, A.; Zhao, J.; Schatz, G. C.; Sligar, S. G.; Van Duyne, R. P. *Anal. Chem.* **2009**, *81*, 3754.

(11) (a) Dubertret, B.; Skourides, P.; Norris, D. J.; Noireaux, V.; Brivanlou, A. H.; Libchaber, A. *Science* **2002**, *298*, 1759. (b) Mulder, W. J. M.; Koole, R.; Brandwijk, R. J.; Storm, G.; Chin, P. T. K.; Strijkers, G. J.; Donega, C. D.; Nicolay, K.; Griffioen, A. W. *Nano Lett.* **2006**, *6*, 1.

(12) (a) Pellegrino, T.; Manna, L.; Kudera, S.; Liedl, T.; Koktysh, D.; Rogach, A. L.; Keller, S.; Radler, J.; Natile, G.; Parak, W. J. *Nano Lett.* **2004**, *4*, 703. (b) Smith, A. M.; Nie, S. M. *Angew. Chem., Int. Ed.* **2008**, *47*, 9916.

(13) (a) Skajaa, T.; et al. *Nano Lett.* **2010**, *10*, 5131. (b) McMahon, K. M.; et al. *Nano Lett.* **2011**, *11*, 1208.

(14) Israelachvili, J. N. *Intermolecular and Surface Forces*, 3rd ed.; Academic Press: Boston, 2011.

(15) (a) Gopalakrishnan, G.; Danelon, C.; Izewska, P.; Prummer, M.; Bolinger, P.-Y.; Geiss-bühler, I.; Demurtas, D.; Dubochet, J.; Vogel, H. *Angew. Chem., Int. Ed.* **2006**, *45*, 5478. (b) Al-Jamal, W. T.; Al-Jamal, K. T.; Tian, B.; Lacerda, L.; Bomans, P. H.; Frederik, P. M.; Kostarelos, K. *ACS Nano* **2008**, *2*, 408.

(16) (a) Johnsson, M.; Edwards, K. *Biophys. J.* **2003**, *85*, 3839. (b) Nagarajan, R. *Langmuir* **2002**, *18*, 31.

(17) Arnspang, E. C.; Brewer, J. R.; Lagerholm, B. C. *PLoS One* **2012**, *7*, e48521.

(18) Jasieniak, J.; Smith, L.; Embden, J. v.; Mulvaney, P.; Califano, M. *J. Phys. Chem. C* **2009**, *113*, 19468.

(19) Smith, A. M.; Nie, S. M. *Nat. Biotechnol.* **2009**, *27*, 732.

(20) (a) Chauhan, V. P.; Popovic, Z.; Chen, O.; Cui, J.; Fukumura, D.; Bawendi, M. G.; Jain, R. K. *Angew. Chem., Int. Ed.* **2011**, *50*, 11417. (b) Lane, L. A.; Qian, X. M.; Smith, A. M.; Nie, S. *Annu. Rev. Phys. Chem.* **2015**, *66*, 521.

DOI: 10.1021/jacs.5b11225
J. Am. Chem. Soc. 2016, 138, 64−67